J. Membrane Biol. 168, 77–89 (1999)

The Journal of
Membrane
Biology

Select *de novo* Gene and Protein Expression During Renal Epithelial Cell Culture in Rotating Wall Vessels is Shear Stress Dependent

J.H. Kaysen[1,4], W.C. Campbell[1], R.R. Majewski[4], F.O. Goda[1], G.L. Navar[1], F.C. Lewis[1,2], T.J. Goodwin[5], T.G. Hammond[1,3,4]

[1]Nephrology Section, Department of Medicine and Tulane Environmental Astrobiology Center, Tulane/Xavier Center for Bioenvironmental Research, 1430 Tulane Avenue, New Orleans, LA 70112, USA
[2]Department of Surgery, Tulane University Medical Center, 1430 Tulane Avenue, New Orleans, LA 70112, USA
[3]New Orleans VA Medical Center, 1601 Perdido St., New Orleans, LA 70146, USA
[4]University of Wisconsin Hospitals and Clinics and William S. Middleton Memorial V.A. Hospital, Madison, WI 53705, USA
[5]NASA, Johnson Space Center, 2101 NASA Road No. 1, Houston, TX 77058, USA

Received: 30 June 1998/Revised: 30 November 1998

Abstract. The rotating wall vessel has gained popularity as a clinical cell culture tool to produce hormonal implants. It is desirable to understand the mechanisms by which the rotating wall vessel induces genetic changes, if we are to prolong the useful life of implants. During rotating wall vessel culture gravity is balanced by equal and opposite hydrodynamic forces including shear stress. The current study provides the first evidence that shear stress response elements, which modulate gene expression in endothelial cells, are also active in epithelial cells. Rotating wall culture of renal cells changes expression of select gene products including the giant glycoprotein scavenger receptors cubulin and megalin, the structural microvillar protein villin, and classic shear stress response genes ICAM, VCAM and MnSOD. Using a putative endothelial cell shear stress response element binding site as a decoy, we demonstrate the role of this sequence in the regulation of selected genes in epithelial cells. However, many of the changes observed in the rotating wall vessel are independent of this response element. It remains to define other genetic response elements modulated during rotating wall vessel culture, including the role of hemodynamics characterized by 3-dimensionality, low shear and turbulence, and cospatial relation of dissimilar cell types.

Key words: Flow cytometry — Antisense oligos — Microgravity — Astrobiology — Differential display

Introduction

The rotating wall vessel is a horizontally rotated cylindrical cell culture device with a coaxial tubular oxygenator [6, 14, 36, 38, 39]. The rotating wall vessel induces expression of select tissue-specific proteins in diverse cells cultures [2, 6, 9, 12, 38]. The mechanisms by which the rotating wall vessel induces tissue-specific protein expression are postulated to be mediated by the provision of unique cell culture hemodynamics characterized by 3-dimensionality, low shear and turbulence and cospatial relation of dissimilar cell types [6, 37, 38]. The genetic mechanisms of rotating wall vessel culture have never before been analyzed.

Rotating wall vessel technology has recently entered clinical medical practice by facilitating pancreatic islet implantation [31, 32]. Pancreatic islets are prepared in rotating wall vessels to maintain production and regulation of insulin secretion. The islets are alginate encapsulated to create a noninflammatory immune haven, and implanted into the peritoneal cavity of Type I diabetic patients. This implantation of pancreatic islets has maintained normoglycemia for 18 months in diabetic patients, and progressed to Phase III clinical trials [31, 32].

Correspondence to: T.G. Hammond

Abbreviations: 2-D, two dimensional; ICAM, intercellular adhesion molecule; IL-1, interleukin 1; MnSOD, magnesium dependent superoxide dysmutase; RWV, rotating wall vessel; STLV, slow turning lateral vessel form of RWV; VCAM, vascular cell adhesion molecule.

There is substantial interest both in applying similar technology to the delivery of numerous other hormones, and prolonging implant life by understanding the mechanisms of rotating wall vessel culture action.

For a deceptively simple system, the engineering definition of the forces active in the rotating wall vessel is far from simple [6, 14, 15, 36, 37, 38]. Cell aggregates fall at terminal velocity in the vessels, with gravity balanced by a complex array of shear, centrifugal and other forces which produce slow spiraling coriolus-induced particle motion. Mathematical modeling of the particle motion in the vessels is sophisticated, but complex and poorly intuitive [6, 14, 36, 38, 39]. In the original analysis of the gravity-induced particle motion in these zero-head-space tissue culture vessels, the interpretation was that at "boundary conditions such vessels simulate microgravity" [37, 38]. The rotating wall vessel delivers a controlled shear stress to the three-dimensional cell aggregates, far less than other shear stress models such as stirred fermentors, but substantially more than conventional 2-dimensional flask or bag cultures [6, 14, 37, 38]. As shear is induced by the movement of cells against a stirring impeller and the vessel wall, these effects are minimized in the rotating wall vessel by reducing impeller size to nonexistent, and rotating the vessel wall with the culture [6, 37, 38].

Our lab is interested, not in rotating wall vessel engineering, but the cell biological mechanisms which mediate changes in gene and protein expression in these vessels. Genetic shear stress response elements are known to mediate changes in endothelial cell gene expression in response to flow [17, 18, 22, 25]. Although many of the classic shear stress response genes such as ICAM, VCAM and MnSOD are also expressed in many epithelial cells, shear stress response elements have not been examined in epithelial cells. This is because the degree of shear employed for gene induction in endothelial cells damages most epithelial cells. The modest shear stress in the rotating wall vessel makes it ideally suited to test if shear stress response elements mediate specific genetic changes in epithelial cells [6, 14].

We chose primary kidney cells as our model system for study as there is an acute need for cultural renal cells expressing differentiated features [9, 13, 24, 26]. Although, the kidney is the source of the hormone erythropoeitin and the active 1-25-dihydroxy form of vitamin D3, no currently available cell line releases these hormones to facilitate regulatory study. The kidney also provides simply identifiable tissue specific markers. Microvilli, with an abundant villin core, are easily detected on electron microscopy.

Several lines of evidence suggest that other easily detected renal markers, the giant glycoprotein receptors, known as megalin and cubulin, mediate common nephrotoxicities [4, 9, 21, 24, 26]. Megalin is a 600 kDa single transmembrane domain glycoprotein receptor [27] recently shown to be a receptor for polybasic drugs including the aminoglycoside antibiotics [20], and the receptor responsible for delivery of vitamin D into renal cells [5]. Cubulin, a 460 kDa receptor, has proven to be the receptor for vitamin B12-intrinsic factor [30] and myeloma light chains [3]. Despite numerous differentiating maneuvers and reagents, there is no currently available renal cell line which expresses megalin or cubulin [9, 24, 26]. This study examines the expression of cubulin, megalin and classic shear stress response genes during rotating wall vessel culture, and the mechanisms mediating induced changes.

Materials and Methods

Cells

Rat Renal Cortical Cells

Rat renal cells were isolated from renal cortex harvested from euthanized Sprague Dawley rats (Harlan Sprague-Dawley, Cleveland, OH) as previously [8]. In brief, renal cortex was dissected out with scissors, minced finely in a renal cell buffer 137 mmol NaCl, 5.4 mmol KCl, 2.8 mmol $CaCl_2$, 1.2 mmol $MgCl_2$, 10 mmol HEPES-Tris, pH 7.4. The minced tissue was placed in 10 ml of a solution of 0.1% Type IV collagenase and 0.1% trypsin in normal saline. The solution was incubated in a 37°C shaking waterbath for 45 min with intermittent titubation. The cells were spun gently (800 rpm for 5 min), the supernatant aspirated, the cells resuspended in 5 ml renal cell buffer with 0.1% bovine serum, and passed through a fine (70 μm) mesh. The fraction passing through the mesh was layered over a discontinuous gradient of 5% bovine serum albumin and spun gently. The supernatant was again discarded. The cells were resuspended in DMEM/F-12 medium (ciprofloxacin and fungizone treated) and placed into culture in various culture vessels in a 5% CO_2 95% O_2 incubator.

Human Renal Cortical Cells

Human renal cortical cells were isolated by Clonetics (San Diego, CA) from kidneys unsuitable for transplantation. Differential trypsinization resulted in cell fractions highly purified for proximal tubular cells compared to the natural mixture of cells in the renal cortex. The coculture of the natural cell mix, and highly purified proximal tubular cells were cultured separately in a growth medium identical to conditions for the rat renal cells.

Culture Techniques

Rotating Wall Vessels

When grown under conventional conditions in DMEM/F12 supplemented with fetal calf serum, and an antibiotic cocktail [ciprofloxacin and fungizone]. Both rat and human cells form a monolayer in conventional T-flask culture. To increase epithelial cell differentiation [6, 28] renal cells were cultured in a rotating wall vessel known as a 55 ml Slow Turning Lateral Vessel (STLV) [6, 28]. The STLV is a horizontally cylindrical culture vessel, turning on its long axis, with a coaxial oxygenator. To initiate cell culture, the STLV was filled with medium,

and seeded by addition of cell suspension (2×10^6 cells/ml). Residual air was removed through a syringe port and vessel rotation was initiated at 10 rotations per min and maintained for 10–16 days. Medium was changed every 2 to 3 days depending on glucose utilization. Concomitant with cells, microcarrier beads were added an 5 mg/ml to promote aggregate formation in the STLV. Without beads the cells became shattered in the vessel in a few hours. Beads were cytodex-3 in all protocols except when electron microscopy was planned when easily sectioned Cultisphere GL beads were utilized.

Stirred Controls

To provide a stirred control, stirred fermentor culture vessels which mix in the horizontal plane were loaded with identical concentrations of cells and beads from the same pool added to the STLV [6, 15, 33].

Static Controls

Gas permeable Fluoroseal bags (Fluoroseal, Urbana, IL) in 7 or 55 ml size were selected as conventional static controls. Culture beads were added to the conventional controls at the same density as the STLV cultures [6, 28].

Electron Microscopy Quantitation of Number of Microvilli

Transmission electron micrographs were performed on cell aggregates from the rotating wall vessels and conventional monolayers. Cells were washed with ice-cold phosphate buffered saline, then fixed for electron microscopy with 2.5% glutaraldehyde in phosphate buffered saline [9, 10]. The samples were then transferred to 1% osmium tetroxide in 0.05 M sodium phosphate (pH 7.2) for several hours, dehydrated in an acetone series followed by embedding in Epon. Lead-stained thin sections were examined and photographed using a Phillips EM/200 electron microscope. For electron microscopy the easily sectioned Cultispere GL beads, replaced Cytodex-3 which are difficult to section.

Flow Cytometry Analysis of Cells and Membranes

Flow cytometry analysis was performed on a Becton Dickinson FACStar flow cytometer using a dedicated Consort 30 computer [8, 9, 10]. Excitation was at 488 nm using a Coherent 5W Argon-ion laser. For each particle, emission was measured using photomultipliers at 530 ± 30 nm and 585 ± 26 nm. Data were collected as 2,000 event list mode files and were analyzed using LYSYS software.

Analysis of the Proximal Tubule Epithelial Marker, γ-Glutamyl Transpeptidase

Cellular enzymes were labeled for flow cytometry analysis on a cell-by-cell basis as previously [8]. To measure γ-glutamyl transpeptidase activity, a γ-glu- derivative of 4-methoxy-β-naphthylamine [4-MNA] (Enzyme System Products, Livermore, CA) was employed. The enzyme specifically cleaves this substrate, liberating free 4-MNA. In the presence of 5-nitrosalicaldehyde (5-NA) at pH 6.0, free 4-MNA is almost instantaneously trapped and precipitated. The product of 4-MNA and 5-NA is fluorescent in the visible spectrum, excited at 488nm with a broad emission spectrum from 510nm through 680nm [7] facilitating simple flow cytometry analysis.

Analysis of the Endosomal Distribution of Megalin and Cubulin by Flow Cytometry

To quantitate the total and endosomal expression of cubulin and megalin in conventional culture, stirred fermentors and STLV rotating wall vessels (SYNTHECON) 0.3 mg/ml 10S fluorescein-dextran was to each cell culture for 10 minutes at 37°C in the CO_2 incubator. This loads an entrapped fluorescent dye into the early endosomal pathway [9, 10]. Cells were then immediately diluted into ice-cold phosphate buffered saline and washed once. Next the cells were homogenized with 6 passes of a tight fitting glass-Teflon motor driven homogenizer. A postnuclear supernatant was formed as the $11{,}000 \times g$ supernatant, $180{,}000 \times g$ pellet of membrane vessels.

Aliquots of membrane vesicles were labeled with megalin or cubulin antisera. The megalin and cubulin antisera are rabbit polyclonals raised to affinity purified and chromatographically pure receptor [21, 26]. Membrane vesicles were first preincubated in 50% normal goat serum for 2 hr to reduce nonspecific binding of secondary antisera raised in goat. After washing aliquots of membrane vesicles were stained with serial log dilution of antisera and incubated at 4°C overnight. After further washing 1:40 of goat anti-rabbit affinity purified rat preabsorbed phycoerthyrein conjugated secondary antiserum was added, and incubated for 4 hr at room temperature. Prior to flow cytometry the membrane vesicles were washed and resuspended in 200 mM mannitol 100 mM KCl, 10 mM HEPES pH 8.0 with Tris to which had been added 10 μM nigericin. In the presence of potassium nigericin collapses pH gradients, ensuring optimal fluorescence of the highly pH dependent fluorescein-dextran emission. Fluorescein-dextran and antibody staining tagged by phycoerythrein were now analyzed and colocalized on a vesicle-by-vesicle basis by flow cytometry.

Two Dimensional Gel Electrophoresis Analysis of Protein Content

Two-dimensional electrophoresis was performed according to the method of O'Farrell [23] by Kendrick Labs (Madison, WI) as follows: Isoelectric focusing was carried out in glass tubes of inner diameter 2.0 mm, using 1% pH 2.5–5 ampholines (LKB Instruments, Baltimore, MD) and 1% pH 4–8 ampholines (BDH from Hoefer Scientific Instruments, San Francisco, CA) for 9600 volt-hrs. One μg of an IEF internal standard, tropomyosin protein, with lower spot M.Wt 33,000 and pI 5.2 was added to the samples. This standard is indicated by an arrow on the stained 2-D gel. After equilibration for 10 min in Buffer "O' (10% glycerol, 50 mM dithiotheitol, 2.3% SDS and 0.625 M Tris, pH 6.8) the tube gels were sealed to the top of a stacking gel which is on top of a 10% acrylamide slab gel (0.75 mm thick). SDS slab gel electrophoresis was then carried out for about 4 hr at 12.5 mA.gel. Proteins standards appear as horizontal lines on the Coomassie Brilliant Blue R-250 stained 10% acrylamide slab gels.

Differential Display

Differential display of expressed genes was compared in aliquots of the same cells grown in a 55 ml rotating wall vessel (STLV) or conventional gas permeable 2-dimensional bag controls. Differential display was performed using Delta RNA Fingerprinting system (Clonetech Labs, Palo Alto, CA). Copies of expressed genes were generated by polymerase chain reaction using random 25 mer primers and separated

on a 6% DNA sequencing gel. Bands of different intensity between control and STLV, representing differentially expressed genes, were identified by visual inspection, excised and reamplified using the same primers. Differential expression and transcript size were confirmed by Northern hybridization. PCR products were then subcloned into the pGEM-T vector (Promega, Madison, WI) and sequenced using fMOL cycle sequencing system (Promega, Madison, WI). Sequences were compared to the Genebank sequences using the BLAST search engine (National Center for Biotechnology Information). For genes of interest the bands were labeled with ^{32}P for confirmation of the changes by Northern blot analysis.

Detection of Gene Expression in Cell Cultures by Semiquantitative RT-PCR

Cell aggregates from the rotating wall vessel or bag cultures were washed once in ice-cold phosphate buffered saline and snap frozen at −70°C until RNA was isolated. Total RNA was isolated using Trizol (GibcoBRL). First strand cDNA was reverse transcribed from 2 μg of total RNA using random primers and Superscript II RT (GibcoBRL). Before cDNAs were subjected to semiquantitative RT-PCR they were normalize by PCR using 18S rRNA primers/copetimers from the QuantumRNA Quantitative RT-PCR Module (Ambion, Austin, TX) and primers for glyceraldehyde 3-phosphate dehydrogenase (GAPDH). Twenty percent of the PCR reaction was electrophoresed on agarose/ethidium bromide gels and visualized under UV light. Electrophoresis results were recorded and quantitated using the Kodak Digital Science 1D Image Analysis Software. Semiquantitative PCR for each gene of interest was performed at two concentrations of cDNA and 28 and 32 cycles of amplification to ensure we made measurements on the initial linear portion of the response curve. A control PCR with GAPDH was also carried out with each cDNA to assure that the input of RNA and reaction efficiencies were all similar. The PCR reactions were electrophoresed and quantitated as described above.

Genetic Decoys

Double stranded genetic decoys matching the sequence of a known shear stress response element were synthesized (Chemicon International, La Jolla, CA) [structure and sequence shown at top of Fig. 4]. These decoys had a terminal phosphothiorate moiety to prevent intracellular lysis, and a phosphodiester backbone to facilitate passage across cell membranes [29]. Passage to and accumulation in the nuclear compartment of cultured cell was confirmed by confocal imaging of a fluorescein tagged decoy. Three decoys were synthesized: the active decoy, a random sequence control in which the six bases of the shear stress response element were scrambles, and a fluorescein conjugated form of the decoy. Decoys were placed in the cell culture medium of rat renal cortical cells grown as above in conventional 2 dimensional culture. Aliquots of cells exposed to control or active sequence decoy at 80 nm concentration were harvested at 2, 6, and 24 hr after exposure.

Genetic Discovery Array

A sample of human renal cortical cells grown in conventional flask culture was trypsinized and split into a gas permeable bag control and a rotating wall vessel (55ml STLV). After 8 days of culture on 5 mg/ml cytodex-3 beads, cells were washed once with ice-cold phosphate buffered saline, the cells were then lysed and mRNA was selected with biotinylated oligo(dT) then separated with streptavidin paramagnetic particles (PolyATtract System 1000, Promega Madison, WI).^{32}P-labeled cDNA probes were then generated by reverse transcription with 32P dCTP. The cDNA probes were hybridized to identical Gene Discovery Array Filters (Genome Systems, St. Louis, MO). The Gene Discovery Array filters contain 18,394 unique human genes from the I.M.A.G.E. Consortium [LLNL] [16] cDNA Libraries which are robotically arrayed on each of a pair of filter membranes. Gene expression was then detected by phosphor imaging and analyzed using the Gene Discovery Software [Genome Systems] [16].

Results

The proportion of proximal tubular cells in human renal cell fractions isolated by differential trypsinization was assayed using an entrapped fluogenic substrate for the proximal enzyme marker γ-glutamyl-transferase [8]. Flow cytometry analysis on a cell-by-cell basis showed rat renal cortical cells were 75 ± 4% ($n = 4$) proximal tubules as determined by flow cytometry analysis of aliquots for the proximal marker γ-glutamyl transferase using Schiff base trapping of cleavage products of L-γ-glu-4-methoxy-4-β-naphthylamine [8]. Flow cytometry analysis of γ-glutamyl-transferase in the natural cell mixture in the human renal cortex to be 85 ± 4%, $n = 4$ proximal tubular cells (Fig. 1*a*, left panel). Following differential trypsinization, and selection of the purist fractions, proximal tubular enrichments as high as 99 ± 1% could be achieved (right panel). As reported in other systems, rotating wall vessels are conductive to cell growth, as evidenced by the rate of glucose consumption assayed as 30 mg/dl glucose/100,000 cells/day in both rotating wall vessel and static control cultures. A cell doubling time of 4 ± 3 days was assayed using Alamar blue in the rotating wall vessel compared to 4 ± 2 days in conventional culture ($n = 4$).

The ultrastructure of cultures of pure proximal tubular cells or renal cortical cell mixtures of human kidneys grown in rotating wall vessels for 16 days were examined by transmission electron microscopy (Fig. 1*b*). Quantitation of the number of microvilli present by counting random plates at the same magnification demonstrates not only that the rotating wall vessel induces microvillus formation, but coculture with the normal mix of renal cortical cells increases the effect. Normal cortical cell mix in conventional 2-D culture has 2 ± 1 microvilli per field ($n = 12$ fields examined); "pure" proximal tubular culture in rotating wall vessel has 10 ± 4 microvilli per field; and the normal cortical cell mix in rotating wall vessel has 35 ± 11 microvilli per field. Figure 1*b* depicts in vivo native rat proximal tubule in upper right panel, conventional culture in upper middle two panels, and STLV culture upper right and lower bay of panels.

To examine the expression of megalin and cubulin in renal cells in culture there are advantages to switch from human to rat cells. Specifically, the rat sequences

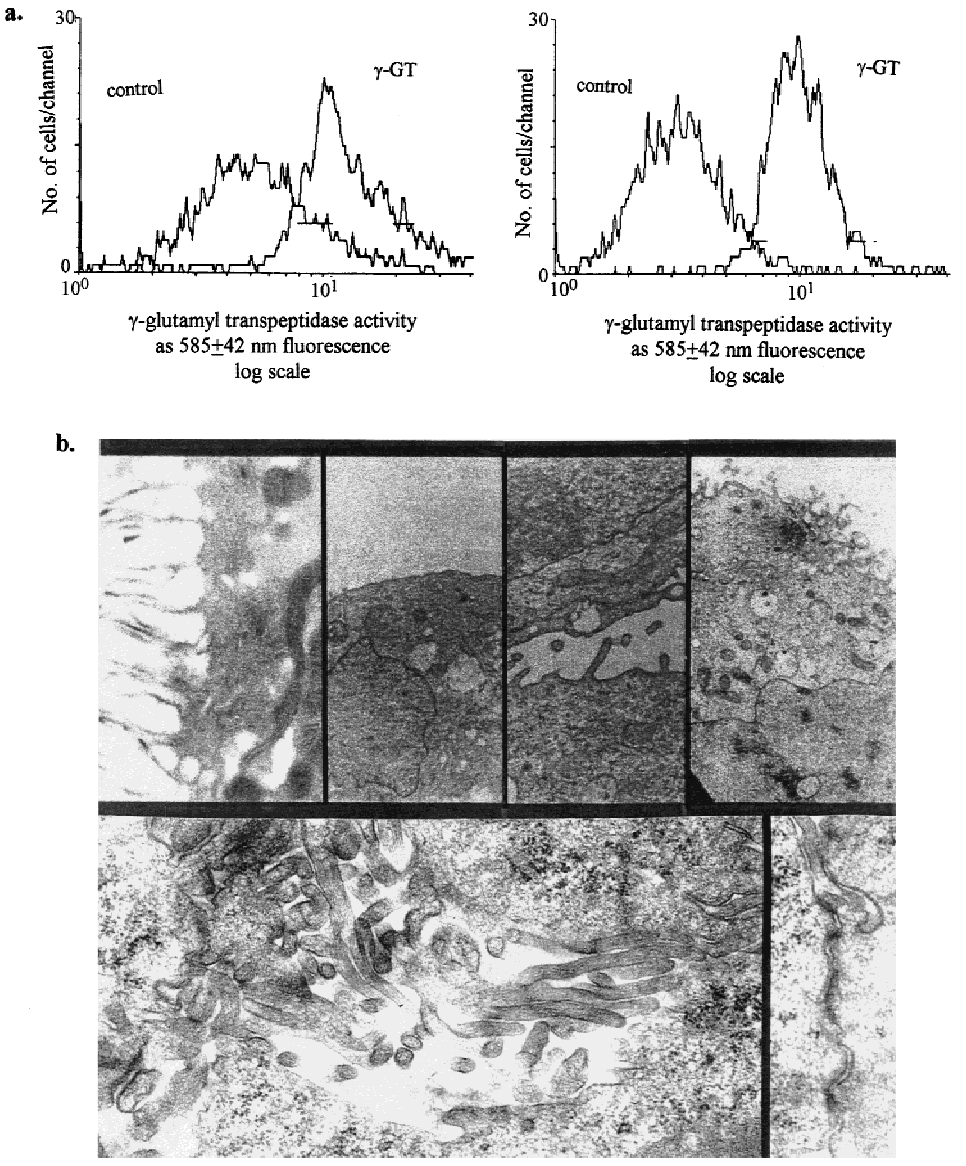

Fig. 1. Homogeneity and structure of human renal epithelial cells in culture. Flow cytometry frequency histograms demonstrate number of cells positive for the proximal tubular marker γ-glutamyl transferase. (*a*) The number of cells with γ-glutamyl transferase activity is shown as the frequency of activity in 2,000 cells compared to an unstained control with trapping agent alone. This is the raw digest of human renal cells (left panel Fig. 1*a*). Following differential trypsinization the percentage of proximal tubular cells present can be increased to 99 ± 1% (right panel Fig. 1*a*). (*b*) Transmission electron micrographs of human epithelial cells in culture. The intact renal cortex in vivo (upper left panel), is compared to the culture of the natural mixture of human renal cortical cells in conventional 2-dimensional culture (upper middle left panel) which is completely devoid of microvilli. Rotating wall vessel culture of pure proximal tubular cells shows some microvilli (upper middle right panel) but there are far more microvilli during rotating wall vessel culture of the natural mix of renal cortical cells (upper right panel). Compared to these representative images, some areas of the natural mixture of cells in the rotating wall vessel show much greater abundance of microvilli (lower left panel), and well defined desmosomes (lower right panel) which are lacking in the other cultures.

of megalin and cubulin have been cloned, while the human sequences have not, and our antisera recognize the rat but not the human isoforms of these proteins. Hence, the natural mixture of cells in the rat renal cortex was placed into culture in rotating wall vessels, stirred fermentors, and traditional culture for analysis of protein expression.

As the endosomal pathway has been implicated to play a central role in the function and pathophysiology of cubulin and megalin we began by colocalizing an entrapped endosomal marker with receptor antibody binding. The ability of flow cytometry to make simultaneous measurements of entrapped fluorescein dextran as an endosomal marker and antibody binding allows construc-

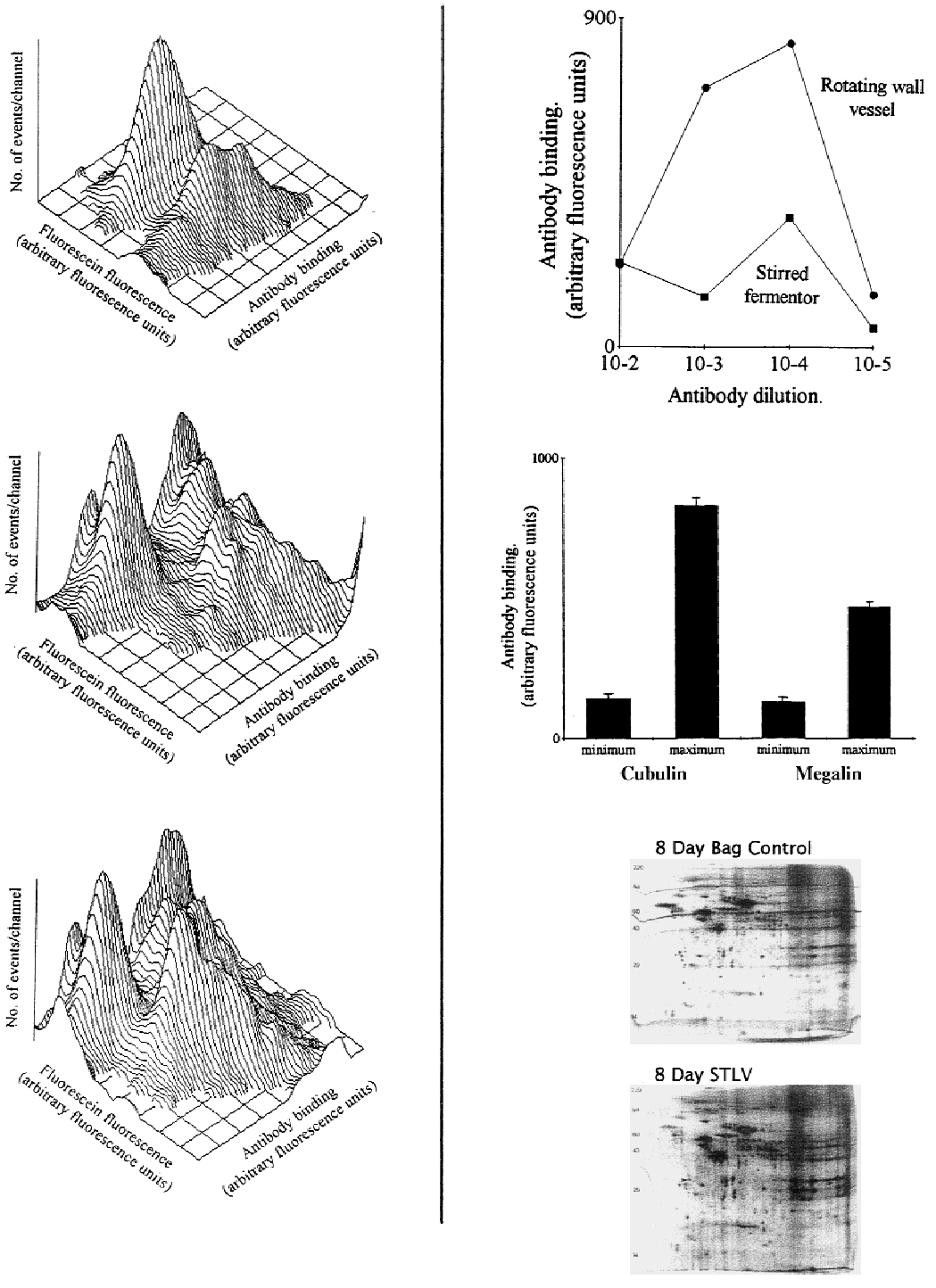

Fig. 2.

tion of three dimensional frequency histograms displaying entrapped fluorescein dextran fluorescence against antibody binding on horizontal axes and number of vesicles in each channel up out of the page (Fig. 2, left column of diagrams). A control sample shows vesicles negative for fluorescein on the left and fluorescein containing endosomes on the right (2000 vesicles depicted, left upper panel). A control without fluorescein entrapped shows only the left population (*not shown*). Co-localization of anti-cubulin binding demonstrates that all the fluorescein positive endosomes are positive for cubulin, while nonendosomal membranes can be subdivided into cubulin positive and negative populations. (left column, middle panel). This pattern is repeated for anti-

Fig. 2. Protein expression in the rotating wall vessel. (*a*) Left column. Analysis of the expression and endosomal compartmentation of megalin and cubulin in renal cells following rotating wall vessel culture. The ability of flow cytometry to make simultaneous measurements of entrapped fluorescein dextran as an endosomal marker and antibody binding allows construction of three-dimensional frequency histograms displaying entrapped fluorescein dextran fluorescence against antibody binding on horizontal axes and number of vesicles in each channel up out of the page. A control sample shows vesicles negative for fluorescein on the left and fluorescein containing endosomes on the right (2000 vesicles depicted upper left panel). A control without fluorescein entrapped shows only the left population (*not shown*). Colocalization of anti-cubulin binding demonstrates that all the fluorescein positive endosomes are positive for cubulin, while nonendosomal membranes can be subdivided into cubulin positive and negative populations (left middle panel). This pattern is repeated for anti-megalin binding in renal cortical cells (left lower panel) [representative of $n = 3$]. (*b*) Right column, upper two panels. Quantitation of cubulin, and megalin antibody binding to renal cell membranes under various culture conditions. Analysis of protein expression in cultured cells by antibody binding used classic serial log dilution antibody curves. An increase in binding with a decrease in dilution is pathognomonic for specific antibody binding during flow cytometry analysis. Binding of anticubulin antisera to membrane vesicles prepared from renal cortical cells after 16 days in culture, detected by the fluorescence of a phycoerthyrein tagged secondary antibody, shows an almost two log increase in binding with antibody dilution (upper left panel). This increased cubulin antibody binding in the cells grown in the rotating wall vessel (STLV) is more than five times the expression seen in stirred fermentors. Similarly there was no detectable expression in the conventional cultures resulting in a flat line (*not shown*). Binding of normal serum and minimal dilution of primary antisera were not detectably different. Binding curves for anti-megalin antiserum showed a similar pattern (*not shown*). Figure 2 (middle right panel) depicts nonspecific (minimum) and peak binding of each antiserum following rotating wall vessel culture [representative of $n = 3$]. (*c*) Right column, lower panels. Two-dimensional SDS-PAGE analysis of protein content of cells following rotating wall vessel culture. Analysis of the protein content of cultures of the natural mixture of rat renal cortical cells after 16 days culture in gas permeable bags as a control (lower right panel) or rotating wall vessel depicts changes in a select set of proteins. Molecular weight (14–220 kDa) on the abscissa is displayed against isoelectric point (pH 3–10) on the ordinate [representative of $n = 2$].

megalin binding in renal cortical cells (left column, lower panel) in culture.

Next, analysis of protein expression in cultured cells by antibody binding used classic serial log dilution antibody curves. An increase in binding with a decrease in dilution is pathognomonic for specific antibody binding during flow cytometry analysis. Binding of anti-cubulin antisera to membrane vesicles prepared from renal cortical cells after 16 days in culture, detected by the fluorescence of a phycoerythyrein tagged secondary antibody, shows an almost two log increase in binding with antibody dilution (Fig. 2, upper right panel). This increase in the cells grown in the rotating wall vessel (STLV) is more than five times the expression seen in stirred fermentors. Similarly there was no detectable expression in the conventional cultures resulting in a flat line (*not shown*). Comparison of maximal binding of the anti-cubulin antibody to a minimum taken to be the antibody dilution at which there is no further decline in signal with primary antibody dilution is shown in Fig. 2, right middle panel. Binding of normal serum and minimal dilution of primary antisera were not detectably different. Binding curves for anti-megalin antiserum showed a similar pattern (*not shown*) but the peak binding was a little lower (Fig. 2, middle panel). Again stirred fermentor has much less expression than the rotating wall vessel (STLV) and the conventional cell membranes have no detectable binding (*not shown*).

To get an idea of the proportion of proteins changing in the rotating wall vessel, we performed two-dimensional gel SDS-PAGE analysis on cultures grown in the rotating wall vessel and bag controls (Fig. 2, lower right panels). This demonstrates changes are in a select group of proteins.

To identify the genes changing during rotating wall vessel culture we performed differential display. Differential display of expressed genes was compared in aliquots of the same rat renal cells grown in a 55 ml rotating wall vessel (STLV) or conventional gas permeable 2-dimensional bag controls. Differential display of copies of expressed genes were generated by polymerase chain reaction using random 25 mer primers and separated on a 6% DNA sequencing gel (Fig. 3, lower left panel). Bands of different intensity between control and STLV, representing differentially expressed genes, were identified by visual inspection, excised and reamplified using the same primers. Differential expression and transcript size were confirmed by Northern hybridization (Fig. 3, lower middle panel). PCR products were then subcloned into the pGEM-T vector and sequenced. Sequences were compared to the Genebank sequences using the BLAST search engine. One expressed gene which decreased in the STLV (band D on gel Fig. 3*a*) was identified as rat manganese-containing superoxide dysmutase (98% match 142 of 144 nucleotides). Two genes which increased in the STLV were confirmed by Northern blot analysis (Fig. 3, lower middle panel). Band A was identified as the interleukin-1 beta gene (100% match for 32 of 32 nucleotides). Band B, a clone of only a few hundred base pairs, corresponded to a 20 kB transcript on a Northern blot, and is an unidentified gene that has a 76% homology to the mouse GABA transporter gene (on BLAST search).

To examine the genetic changes in specific genes we examined the expression of tissue specific epithelial cell markers, and classic shear stress response dependent genes by RT-PCR (Fig. 3). Several genes specific for renal proximal tubular epithelial cells, including mega-

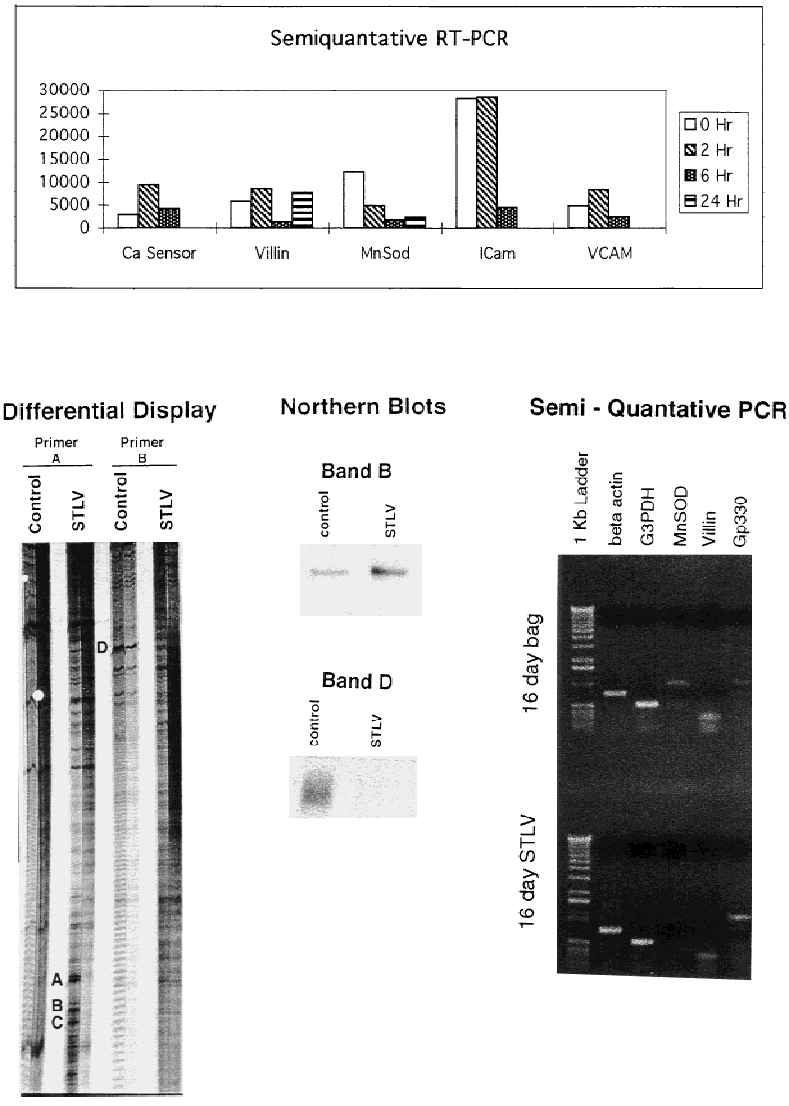

Fig. 3. Gene expression in the rotating wall vessel. (*a*) Upper panel. Differential display of genetic expression of rat renal cortical cells grown in conventional culture or rotating wall vessels. Differential display of expressed genes was compared in aliquots of the same cells grown in a 55 ml rotating wall vessel (STLV) or conventional gas permeable 2-dimensional bag controls. For differential display copies of expressed genes were generated by polymerase chain reaction using random 25 mer primers and separated on a 6% DNA sequencing gel (lower left panel). Bands of different intensity between control and STLV, representing differentially expressed genes, were identified by visual inspection, excised and reamplified using the same primers. Differential expression and transcript size were confirmed by Northern hybridization (lower middle panel). PCR products were then subcloned into the pGEM-T vector and sequenced. Sequences were compared to the Genebank sequences using the BLAST search engine. One expressed gene which decreased in the STLV (band D on gel above) was identified as rat manganese-containing superoxide dysmutase (98% match 142 of 144 nucleotides). Two genes which increased in the STLV, band A was identified as the interleukin-1 beta gene (100% match for 32 of 32 nucleotides) and Band B which corresponded to a 20 kB transcript on a Northern blot appears to be a unidentified gene that has a 76% homology to the mouse GABA transporter gene (lower middle panel). (*b*) Lower right panel. RT-PCR of time dependent change in genes during rotating wall vessel culture. Semiquantitative RT-PCR shows acute time dependent in the epithelial genes extracellular calcium sensing receptor (Ca Sensor), villin and the shear stress response element genes MnSOD, ICAM, and VCAM. (upper panel). There is no change in β-actin or GADPH. Unlike in endothelial cells many of these changes are prolonged as at 16 days MnSOD, villin and megalin (Gp330) changes persist (lower right panel) [representative of $n = 3$].

lin, cubulin, the extracellular calcium sensing receptor (Ca Sensor), and the microvillar structural protein villin, increase early in rotating wall vessel culture (Fig. 3 upper panel). Similarly there were dynamic time-dependent changes in classic shear stress-dependent genes including ICAM which increased, and MnSOD and VCAM which were suppressed. Many but not all of these changes were prolonged, as after 16 days in culture gene expression of megalin (Gp330) is still elevated, MnSOD is still suppressed while villin is back at control levels (Fig. 3 lower right panel). Expression of control GADPH, β-actin and 18S genes did not change throughout the time course.

To test for a role of a putative endothelial shear stress response element in these renal cortical cell changes, we synthesized an antisense probe for the sequence (Fig. 4, upper panel). A control probe had the active motif scrambled. Confocal imaging of a fluorescein conjugated form of the probe confirmed nuclear delivery of the probe (*images not shown*). Culture of rat renal cortical cells in 80 nm of the probe, resulted in a time dependent decrease in MnSOD, but no change in villin gene expression (Fig. 4 lower panels). Gene expression in cells receiving no treatment (NT) was no discernibly different from cells treated with a scrambled sequence control probe (control).

To confirm the genetic responses to rotating wall vessel culture, and return the analysis to human cells we performed automated gene display analysis of expressed RNA on human renal cortical cells grown in a control gas-permeable bag and the STLV for 8 days [16]. Of the more than 18,000 genes assayed a select group was again observed to change (Fig. 5). In particular, vectored changes in all the classic shear stress response genes we

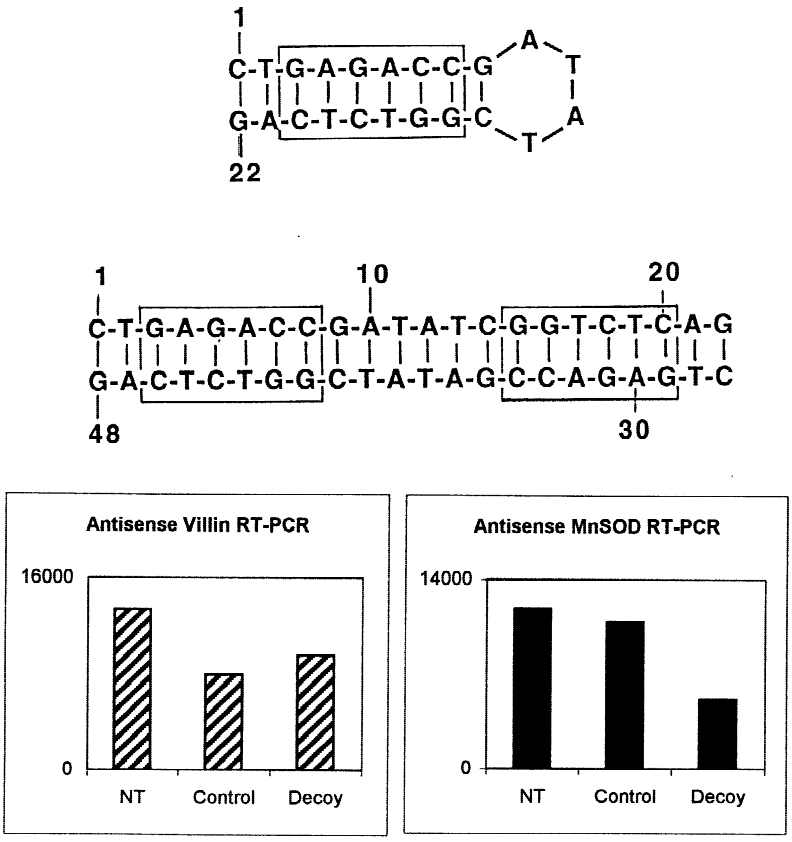

Fig. 4. Structure and effects of antisense probe for shear stress response element on rat renal cortical epithelial cells. (*a*) upper panel. Structure. The probe with sequence CTGAGACCGATATCGGTCTCAG has two possible conformations. As a single strand it would fold back on itself to form a binding element for the transcription factor. As a double strand it would then have two binding sites for the transcription factor, one in the sense orientation and one in the antisense orientation. (*b*) Lower panel. Effects of antisense shear stress response element probe on time dependent gene expression. The antisense probe added to conventional 2-dimensional cultures of rat renal cortical cells at 80 nm decreases MnSOD in a time dependent manner. Comparison is made to controls with the active binding site scrambled (control) and cells receiving no treatment (NT). In contrast to effects on MnSOD, the antisense probe for a known shear stress response element has no effect on villin gene expression [representative of $n = 3$].

assayed by RT-PCR and differential display in rat cell culture were confirmed. A battery of tissue-specific genes was increased including villin, angiotensin converting enzyme, parathyroid hormone receptor and sodium channels. Other physical force dependent genes such as heat shock proteins 27/28 kDa and 70-2 changed, as did focal adhesion kinase, and a putative transcription factor for shear stress responses NF-κβ. Fusion proteins such as synaptobrevin 2 show mildly decreased gene expression. Several cytoskeleton proteins such as clathrin light chains have continued change at steady state, consistent with the dramatic structural changes observed. Last, several transcription factors undergo large changes in gene expression, although their role remains to be defined.

Discussion

The rotating wall vessel bioreactor provides quiescent colocalization of dissimilar cell types [6, 33]; mass transfer rates that accommodate molecular scaffolding; and a micro-environment that includes growth factors [6, 33]. Engineering analysis of the forces active in the vessel is complex [6, 14, 36, 37, 38]. This study provides the first evidence for the cell biological mechanisms by which the vessel induces changes in tissue specific gene and protein expression.

There are two possible explanations why the rotating wall vessel induces an order of magnitude more expression of the renal toxin receptors cubulin and megalin than stirred fermentor culture. First, there are dramatic differences in the degree of shear stress induced. The rotating wall vessel induces 0.5–1.0 dynes/cm^2 shear stress [6], while stirred fermentors induce 2–40 dynes/cm^2 depending on design and rotation speed [6, 14, 33]. This degree of stress damages or kills most epithelial cells [6, 14, 33]. Second, impeller trauma in the stirred fermentor, is absent in the rotating wall vessel. This explains why there was far more cubulin and megalin induced in renal cultures in rotating wall vessel culture than a stirred fermentor. Neither receptor was detectable in conventional 2-dimensional culture.

Rotating wall vessel culture induced changes in a select set of genes, as evidenced by the genetic differential display gels, the 2-dimensional protein gel analysis, and robotic automated gene display. We can interpret mechanistic information from knowledge of the pattern of response and distribution of certain gene products.

Megalin and cubulin represent the first pattern of change, as these proteins are restricted in distribution to renal cortical tubular epithelial cells. The increase in megalin mRNA and protein, and cubulin protein expression is therefore unequivocal evidence for changes in the epithelial cells. This provides an important new tool for studies of nephrotoxicity. Long suspected to play a role

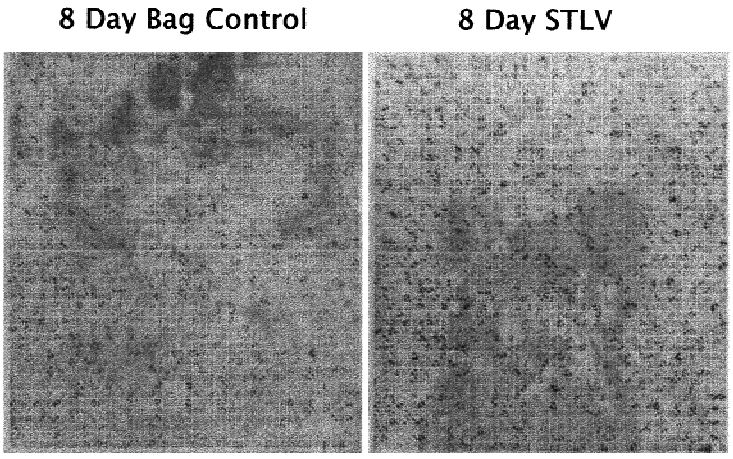

Bag Int	STLV int	Score	Ratio	Int. Diff	GB Acc	SSRE Containing Genes
1785.57	623.4	3328.754	2.864	-1162.17	AA143155	superoxide dismutase 2, (MnSOD)
766.39	2443.26	5345.908	3.188	1676.87	N36944	c-fos
365.26	657.05	524.883	1.799	291.79	H07071	vascular cell adhesion molecule
1156.27	1020.21	154.212	1.133	-136.06	R71741	intercellular adhesion molecule 1
0	2.85	28.422	9.999	2.84	AA187144	endothelin 1
349.28	559.27	336.252	1.601	210	AA130550	transforming growth factor beta
788.01	383.91	829.417	2.053	-404.09	AA203337	platelet-derived growth factor receptor, beta
627.81	452.26	243.674	1.388	-175.54	R75975	monocyte chemotactic protein 1
485.05	218.86	589.982	2.216	-266.2	H67165	nitric oxide synthase 2 (e-nos)
						Renal Epithelium Specific Genes
52.04	17.08	106.522	3.047	34.96	AA074396	Villin
785.8	434.8	634.358	1.807	-351	H03529	AT1 A
6.2	393.73	3874.909	9.999	387.53	H74171	Angiotensin Converting enzyme
602.69	80.35	3918.078	7.501	-522.34	AA211081	sodium channel 1
38.05	425.19	3871.055	9.999	387.14	T78351	parathyroid hormone receptor
625.42	214.97	1194.112	2.909	-410.45	AA206392	Sodium Channel Amoilride Sensitive
552.69	248.03	678.933	2.228	-304.67	H39033	sodium channel, voltage-gated
						Transcription Factors
0	339.2	3391.62	9.999	339.2	T774450	transcription factor E2F
0	64.53	645.305	9.999	64.54	AA136344	heat shock factor 2
297.09	134.76	357.811	2.204	-162.32	R86053	transcription factor NF-kappa-B
0	26.95	269.434	9.999	26.95	AA197291	octamer-binding transcription factor 3
57.49	651.78	5942.207	9.999	594.28	AA039452	GLI-Krueppel related protein
						Cytoskeleton & Motility Proteins
371.51	29.89	3415.744	9.999	-341.61	H70044	protein kinase, calcium/calmodulin-dependent
5.51	555.9	5503.305	9.999	550.39	AA054501	guanine nucleotide-binding protein G25K
328.84	19.66	3091.475	9.999	-309.18	AA180004	Kinesin heavy chain
126.53	13.68	1043.541	9.247	-112.85	AA147847	Vimentin
						Others Genes of Intrest
317.75	847.74	1414.005	2.668	529.99	AA043909	focal adhesion kinase
1195.88	709.7	819.254	1.685	-486.19	AA115776	heat shock protein, 27/28 kDa
0	289.79	2897.539	9.999	289.78	T74240	Heat shock HSP70-2
43.97	0	439.591	9.999	-43.96	T61965	synaptobrevin 2
142.74	847.07	4179.592	5.934	704.32	AA099193	clathrin, light polypeptide a

Fig. 5. Bag Int: The Average normalized intensity for the two points for this clone found on the bag filter
STVL Int: The Average normalized intensity for the two points for this clone found on the STLV filter
Score: The Ratio times the absolute Int. Diff are multiplied to give the score. This is the value used to rank the various hits.
Ratio: This is the Ratio of the average normalized intensities of the two filters for each spot. This is only listed for values greater than 1. The maximum is set at 9.999 which occurs when the normalized spot in one filter is zero, but the normalized intensity of the second spot is large.
Int. Diff: Intensity Differential. This is the difference between the two average normalized intensities.
GB Acc: GenBank Accession number
SSRE: Shear stress response element
Bag Int: The Average normalized intensity for the two points for this clone found on Bag filter.
STLV Int: The Average normalized intensity for the two points for this clone found on STLV filter
Score: The Ratio times the Int. Diff are multiplied to give the score. This is the value used to rank the various hits.
Ratio: This is the Ratio of the average normalized intensities of the two filters for each spot. This is only listed for values greater than 1. The maximum is set at 9.999 which occurs when the normalized spot in one filter is zero, but the normalized intensity of the second spot is large.
Int. Diff: Intensity Differential: This is the absolute difference between the two average normalized intensities.

in renal toxicity, the tissue restricted giant glycoprotein receptors megalin and cubulin, have recently been shown directly to be receptors for common nephrotoxins. Megalin [27] is a receptor for polybasic drugs such as the aminoglycoside antibiotic gentamicin [20] and vitamin D binding protein [5], and cubulin is the receptor for vitamin-B12 intrinsic factor [30], and myeloma light chains [3]. Although these receptors are expressed by transformed placental cells in culture [9, 26], there is currently no renal model expressing these markers for toxicology investigations [24]. Rotating wall culture provides a fresh approach to expression of renal specific markers in culture for study on the pharmacology, biochemistry and toxicology which define the unique properties and sensitivities of renal epithelial cells.

The second pattern of change is represented by villin. Message for the microvilli protein villin increases in the rotating wall vessel in the first day of culture, and we soon observed reformation of microvilli. A decoy matching the nuclear binding motif of a putative shear stress response element failed to induce similar changes. Although the promoter for villin has not been cloned, this suggests the changes in villin were induced by other transcription factors which may be due to shear stress or other stimuli in the bioreactor. Villin is also restricted to brush border membranes such as renal proximal tubular cells, or colonic villi [1, 4]. The observed increases in villin message resolved after 16 days of rotating wall vessel culture.

MnSOD represents a third pattern of response: a mitochondrial enzyme, ubiquitous is distribution, modulated by the classic shear stress response element in endothelial cells [25, 34]. MnSOD message decreased early in the first day of rotating wall vessel culture, and this was persistent after 16 days in culture. These changes were confirmed both when MnSOD was identified as suppressed in the differential display analysis of gene changes, and Northern blot confirmation performed, as well as on robotic gene display analysis. As would be predicted a decoy for the classic shear stress response element induced a decrease in MnSOD. Other shear stress response element dependent genes, specifically, ICAM and VCAM had changes in the rotating wall vessel opposite to MnSOD, mirroring observations made during flow induced stress in endothelial cells [25, 34]. This provides four lines of evidence consistent with a role for shear stress as one mediator of genetic changes induced in the rotating wall vessel.

Differential display of the genes activated and deactivated under rotating wall vessel culture conditions showed rotating wall vessel culture is associated with decreased expression of manganese dependent superoxide dismutase mRNA and increased expression of interleukin-1 β gene mRNA. This greatly extends and brings together previous observations on the interactions of stress, manganese dependent superoxide dismutase expression and interleukin-1. Topper et al. [34] report that an oppositely directed effect: differential display of vascular endothelial cells exposed to high stress demonstrates increased manganese dependent superoxide dismutase gene expression. Other direct evidence links superoxide dismutase and interleukin-1 as increases in manganese superoxide dismutase decrease interleukin-Iα levels in HT-1080 fibrosarcoma cells [19]. In more indirect evidence over expression of mitochondrial manganese superoxide dismutase promotes the survival of tumor cells exposed to interleukin-1 [11]. The current study provides direct evidence that modest shear stress decreases MnSOD in association with an inverse effect on interleukin-1.

Our data demonstrate internal consistency. The changes in MnSOD were observed on differential display, confirmed by Northern blot analysis, and matched responses were detected by both RT-PCR and robotic gene discovery analysis. Megalin demonstrated matched changes in RT-PCR gene and protein expression. Changes in villin observed by RT-PCR were associated with dramatic reformation of microvilli, in which villin is a major structural protein. Although semiquantitative RT-PCR is prone to inherent variation due to the massive amplification of signals, the use of multiple controls which remain unchanged (β-actin, GAPDH and 18S), and experimental confirmation that reactions were linearly related to cDNA concentration, minimizes these problems. The internally consistent findings by other methods strongly suggests our RT-PCR data is valid.

Study of the mechanisms of action of the rotating wall vessel to induce gene and protein expression during cell culture has been hampered by nomenclature. First, the attachment of the moniker “simulated microgravity,” based on engineering analysis of boundary conditions, clouds intuitive analysis of the cell biology as there is no cellular equivalent for this term [6, 36, 37, 38]. Similarly the reduced shear stress in the rotating wall vessel compared to stirred fermentors lead to the term “reduced shear stress culture” [6], whereas there is increased shear stress compared to conventional 2-dimensional culture [6, 14]. We hope that this article is the beginning of a transition from engineering analysis to investigation of mechanisms of biological response in the rotating wall vessel. As cell aggregates remain suspended in the rotating wall culture vessels, gravity is balanced by an equal and opposite force. We document several lines of evidence that shear stress responses are one of the component of the biological response. This opens the door for analysis of other biological response mediators in the vessels, and investigation as to whether unloading of gravity plays as big a role as the oppositely directed balancing forces.

Using the rotating wall vessel as a tool, this data

provides the first evidence that shear stress response elements, which modulate gene expression in endothelial cells, are also active in epithelial cells. As the rotating wall vessel gains popularity as a clinical tool to produce hormonal implants it is desirable to understand mechanisms by which it induces genetic changes [31, 32], if we are to prolong the useful life of implants. We provide several lines of evidence that shear stress response elements are the first mechanism identified by which the rotating wall vessel induces genetic changes. Using a putative endothelial cell shear stress response element binding site as a decoy, we validate the role of this sequence in the regulation of selected genes. However, many of the changes observed in the rotating wall vessel are independent of this response element. The rotating wall vessel provides a quiescent culture modality characterized by near optimal 3-dimensionality, reduction of shear and turbulence, and cospatial relation of dissimilar cell types. It remains to define other genetic response elements modulated during rotating wall vessel culture, to delineate mechanisms of tissue differentiation and engineering in this vessel.

Supported by National Institutes of Health First Award DK46117 (TGH), NIH R21 RR12645 (JHK), and NASA NRA Grants 9-811 Basic and NAG 8-1362 (TGH; TJG). TGH is the recipient of a Veteran's Administration Research Associate Career Development Award. Some of the flow cytometry was performed at the Wisconsin Comprehensive Cancer Center. We thank Grayson Scott of the Core Electron Microscopy Facility at the University of Wisconsin-Madison for transmission electron microscopy analysis.

References

1. Arpin, M.E., Pringault, J., Finidori, A., Garcia, J., Jeltsch, M., Vandekerckhove, J., Louvard, D. 1988. Sequence of human villin: a large duplicated domain homologous with other actin-serving proteins and a unique small carboxy-terminal domain related to villin specificity. *J. Cell Biol.* **107:**1759–1766
2. Baker, T.L., Goodwin, T.J. 1997. Three-dimensional culture of bovine chondrocytes in rotating wall vessel. *In Vitro Cell Dev. Biol.* **33:**358–365
3. Batuman, V., Simon, E., Verroust, P.J., Pontillon, F., Lyles, M., Bruno, J., Hammond, T.G. 1998. Myleoma light chains are ligand for cubulin(gp280). *Am. J. Physiol.* **275:**F246–F254
4. Chantret, I., Barbat, A., Dussaulx, E., Brattain, M.G., Zweibaum, A. 1988. Epithelial polarity, villin expression, and enterocytic differentiation of cultured human colon carcinoma cells: A survey of twenty cell lines. *Cancer Res.* **48:**1936–1942
5. Christensen, E.I., Nykjar, A., Vorum, H., Jacobsen, C., Willnow, T. 1997. Megalin mediates endocytosis of vitamin D-binding protein and thereby reabsorption of vitamin D in renal proximal tubule. *JASN* **8:**59*A* (*Abstr.*)
6. Goodwin, T.J., Prewett, T.L., Wolf, D.A., Spaulding, G.F. 1993. Reduced shear stress: a major component in the ability of mammalian tissues to form three-dimensional assemblies in simulated microgravity. *J. Cell Biochem.* **51:**301–311
7. Goodwin, T.J., Schroeder, W.F., Wolf, D.A., Moyer, M.P. 1993. Rotating-wall vessel coculture of small intestine as a prelude to tissue modeling: aspects of simulated microgravity. *Proc. Soc. Exp. Biol. Med.* **202:**181–192
8. Hammond, T.G. 1992. Analysis and isolation of renal proximal tubular cells using flow cytometry. *Kidney Int.* **42:**997–1005
9. Hammond, T.G., Goda, F.O., Navar, G.L., Campbell, W.C., Majewski, R.R., Galvan, D.L., Pontillon, F., Kaysen, J.H., Goodwin, T.J., Paddock, S.W., Verroust, P.J. 1998. Membrane potential mediates H^+-ATPase dependence of "degradative pathway" endosomal fusion. *J. Membrane Biol.* **162:**157–167
10. Hammond, T.G., Majewski, R.R., Moore, D.J., Schell, K., Morrissey, L.W. 1993. Forward scatter pulse width signals resolve multiple populations of endosomes. *Cytometry* **14:**411–420
11. Hibose, K., Longo, D.L., Oppenheim, J.J., Matsushima, K. 1993. Overexpression of mitochondrial manganese superoxide dismutase promotes the survival of tumor cells exposed to interleukin-1, tumor necrosis factor, selected anticancer drugs, and ionizing radiation. *FASEB J.* **7:**361–368
12. Jessup, J.M., Goodwin, T.J., Spaulding, G. 1993. Prospects for use of microgravity-based bioreactors to study three-dimensional host-tumor interactions in human neoplasias. *J. Cell Biochem.* **51:**290–300
13. Kanazawa, T., Hosick, H.L. 1992. A co-culture system for studies of paracrine effects of stromal cells on the growth of epithelial cells. *J. Tiss. Cult. Meth.* **14:**59–62
14. Kleis, S.J., Schreck, S., Merem, R.M. 1990. A viscous pump bioreactor. *Biotech. & Bioeng.* **36:**771–777
15. Langer, R., Vacanti, J.P. 1993. Tissue engineering. *Science* **260:**920–926
16. Lennon, G.G., Auffray, C., Polymoropoulos, M., Soares, M.B. 1996. The I.M.A.G.E. Consortium: an integrated molecular analysis of genomes and their expression. *Genomics* **33:**151–152
17. Lin, M.C., Almus-Jacobs, F., Chen, H.H., Parry, G.C.N., Mackman, N., Shyy, J.Y.J. 1997. Shear stress induction of the tissue factor gene. *J. Clin. Invest.* **99:**737–744
18. Malek, A.M., Izumo, S. 1995. Control of endothelial cell gene expression by flow. *J. Biomechanics* **28:**1515–1528
19. Melendez, J.A., Davies, K.J.A. 1996. Manganese superoxide dismutase modulates interleukin-Iα levels in HT-1080 fibrosarcoma cells. *J. Biol. Chem.* **271(31):**18898–18903
20. Moestrup, S.K., Cui, S., Vorum, H., Bregengaard, C., Bjørn, S.E., Norris, K., Gliemann, J., Christensen, E.I. 1995. Evidence that epithelial glycoprotein 330/megalin mediates uptake of polybasic drugs. *J. Clin. Invest.* **96:**1404–1413
21. Moestrup, S.K., Kozyraki, R., Christiansen, M., Kaysen, J.H., Rasmussen, H.H., Brault, D., Pontillon, F., Galcoran, M., Christensen, E.I., Hammond, T.G., Verroust, P.J. 1998. The intrinsic factor-vitamin B12 receptor/target of teratogenic antibodies is a megalin-binding peripheral membrane protein with homology to developmental control proteins. *J. Biol. Chem.* **273:**5235–5242
22. Nagel, T., Resnick, N., Atkinson, W.J., Dewey, C.F. Jr., Gimbrone, M.A. Jr. 1994. Shear stress selectively upregulates intracellular adhesion molecule-1 expression in cultured human vascular endothelial cells. *J. Clin. Invest.* **94:**885–891
23. O'Farrell, P.H. 1971. High resolution two-dimensional electrophoresis of proteins. *J. Biol. Chem.* **250:**4007–4021
24. Orlando, R.A., Farquhar, G. 1993. Identification of a cell line that expresses a cell surface and a soluble form of the megalin/receptor-associated protein (RAP) Heymann nephritis antigenic complex. *PNAS USA* **90:**4082–4086
25. Resnick, N., Gimbrone, M.A. Jr. 1995. Hemodynamic forces are complex regulators of endothelial gene expression. *FASEB J.* **9:**874–882
26. Sahali, D., Mulliez, N., Chatelet, F., Laurentwinter, C., Citadelle, D., Sabourin, J.C., Roux, C., Ronco, P., Verroust, P.J. 1993. Com-

parative immunochemistry and ontogeny of two closely related coated pit proteins—the 280kd target of teratogenic antibodies and the 330-kd target of nephritogenic antibodies. *Am. J. Pathol.* **142:**1654–1667

27. Saito, A., Pietromonaco, S., Loo, A.K.C., Farquhar, M.G. 1994. Complete cloning and sequencing of rat megalin/"megalin," a distinctive member of the low density lipoprotein receptor gene family. *Proc. Natl. Acad. Sci. USA* **91:**9725–9729
28. Schwarz, R.P., Goodwin, T.J., Wolf, D.A. 1992. Cell culture for three-dimensional modeling in rotating-wall vessels: an application of simulated microgravity. *J. Tiss. Cult. Meth.* **14:**51–58
29. Schlingensiepen, R. 1997. Antisense—From Technology to Therapy. R. Schlingensiepen, W. Brysch, and W.H. Schlingensiepen, editors. pp. 3–29 Blackwell Science
30. Seetharam, B., Christensen, E.I., Moestrup, S.K., Hammond, T.G., Verroust, P.J. 1997. Identification of rat yolk sac target protein of teratogenic antibodies, gp280, as intrinsic factor-cobalamin receptor. *J. Clin. Invest.* **99:**2317–2322
31. Soon-Shiong, P., Heintz, R.E., Merideth, N., Yao, Q.X., Yao, Z., Zheng, T., Murphy, M., Moloney, M.K., Schmehl, M., Harris, M., Mendez, R., Mendez, R., Sandford, P. 1994. Insulin Independence in a type I diabetic patient after encapsulated islet transplantation. *The Lancet* **343:**950–951
32. Soon-Shiong, P., Feldman, E., Nelson, R., Heintz, R., Yao, Q., Yao, Z., Zheng, T., Merideth, N., Skjak-Brack, G., Espevik, T., Smidsrod, O., Sandford, P. 1993. Long-term reversal of diabetes by the injection of immunoprotected islets. *PNAS USA* **90:**5843–5847
33. Spaulding, G.F., Jessup, J.M., Goodwin, T.J. 1993. Advances in cellular construction. *J. Cell Biochem.* **51:**249–251
34. Topper, J.N., Anderson, K.R., Gimbrone, M.A. Jr. Molecular genetic analysis of shear stress induced endothelial phenotypes. *J. Vasc. Res.* **33:**S100*A* (*Abstr.*)
35. Tuttle, R., O'Leary, D.D.M. 1993. Cortical connections in cocultures. *Curr. Opin. Cell Biol.* **3:**70–72
36. Unsworth, B.R., Lelkes, P.I. 1998. Growing tissues in microgravity. *Nature Medicine* **4(8):**901–907
37. Wolf, D.A., Schwarz, R.P. 1991. Analysis of gravity-induced particle motion and fluid perfusion flow in the NASA-designed rotating zero-head-space tissue culture vessel. *NASA Technical Paper 3143*
38. Wolf, D.A., Schwarz, R.P. 1992. Experimental measurement of the orbital paths of particles sedienting within a rotating viscous fluid as influenced by gravity. *NASA Technical Paper 3200*
39. Zhau, H.E., Goodwin, T.J., Chang, S-M., Baker, T.L., Chung, L.W.K. 1997. Establishment of a three-dimensional human prostate organoid coculture under microgravity-simulated conditions: evaluation of androgen-induced growth and PSA expression. *In Vitro Cell Dev. Biol.* **33:**375–380